FACTA UNIVERSITATIS
Series: **Mechanical Engineering** Vol. 15, Nº 1, 2017, pp. 63 - 71
DOI: 10.22190/FUME170222003L

Original scientific paper

NORMAL LINE CONTACT OF FINITE-LENGTH CYLINDERS

UDC 539.3

Qiang Li, Valentin L. Popov

Department of System Dynamics and the Physics of Friction,
Berlin Institute of Technology, Berlin, Germany

Abstract. *In this paper, the normal contact problem between an elastic half-space and a cylindrical body with the axis parallel to the surface of the half-space is solved numerically by using the Boundary Element Method (BEM). The numerical solution is approximated with an analytical equation motivated by an existing asymptotic solution of the corresponding problem. The resulting empirical equation is validated by an extensive parameter study. Based on this solution, we calculate the equivalent MDR-profile, which reproduces the solution exactly in the framework of the Method of Dimensionality Reduction (MDR). This MDR-profile contains in a condensed and easy-to-use form all the necessary information about the found solution and can be exploited for the solution of other related problems (as contact with viscoelastic bodies, tangential contact problem, and adhesive contact problem.) The analytical approximation reproduces numerical results with high precision provided the ratio of length and radius of the cylinder are larger than 5. For thin disks (small length-to-radius ratio), the results are not exact but acceptable for engineering applications.*

Key Words: *Line Contact, Boundary Element Method, Finite-length Cylinder, Contact Stiffness, Method of Dimensionality Reduction*

1. INTRODUCTION

The contact problem of cylinders with parallel axes or of a flat elastic body with a “lying” cylinder is very common in practical engineering applications, in particular in mechanical elements such as roller bearings, gears and cams [1, 2]. In contrast to the Hertz-like contacts of bodies with curvature in two directions which in engineering mechanics are called “point contacts”, the contact of two parallel cylinders is denoted as a “line contact”. Being an immediate two-dimensional analog of the Hertz contact, the line contact between cylinders with parallel axes is one of basic problems in contact mechanics.

Received February 22, 2017 / Accepted March 15, 2017
Corresponding author: Valentin L. Popov
Department of System Dynamics and the Physics of Friction, Berlin Institute of Technology, Str. des 17 Juni 135, 10623 Berlin, Germany
E-mail: v.popov@tu-berlin.de

Even if the effective dimensionality of a line contact is lower than that of the point contact (2D vs. 3D), the line contact is in some sense more complicated than its 3D analog since in the line contact the "indentation depth" cannot be defined unambiguously. This is related to the logarithmic divergence of the 2D fundamental solution in infinity. In other words, the properties of a 2D contact (line contact) are not "local" but depend on the macroscopic shape of the body. This dependence, however, is relatively weak (logarithmic). Therefore, there exist a large number of approximated solutions [3-5], which have been applied in many further studies, for example in elastic hydrodynamic lubrication [6, 7]. The main structure of all approximate solutions is relatively simple: it reproduces the logarithmic divergence and cuts it up at some characteristic distance, at which the contact ceases to be a line-contact. In the case of a true 2D contact, this is the size of the system (e.g. the radius of contacting cylinders).

On the other hand, for any finite contact, e.g. that of a lying cylinder of finite length, the indentation depth can be determined unambiguously. The macroscopic length which in this case limits the "two-dimensionality" of the line contact is the length of the cylinder. One can anticipate that the indentation depth at a given force will be a weak logarithmic function of the cylinder length. Finding the exact form of this function is the main goal of this paper.

As the solution of the underlying two-dimensional contact problem gives the basis for our consideration, we first provide a brief overview of earlier works on this topic. The contact of cylinders with parallel axes was early studied by Prescott [8] and Thomas and Hoersch [9], and later also investigated by many researchers, for example Lundberg et al. [10]. A good review of analytical solution for this contact problem can be found in Norden's report [11], where the deviation of relationship between the normal load and the indentation depth is given in detail; this relationship is still widely used today. The same analysis is also presented in Puttock and Thwaite's report [12]. In these solutions, the existing result of pressure distribution for elliptical contact is used for cylindrical contact with parallel axes by assuming one axis of ellipse is infinitely large, and then the contact area is considered as a finite rectangle whose length is much larger than its width. For further reference, here we reproduce their solution of a cylinder with radius R and length L pressed into elastic half space under normal load F [12]: the half width of contact rectangle b is equal to:

$$b=\sqrt{\frac{4RF}{\pi E^{*}L}} \tag{1}$$

and indentation depth d is:

$$d=\frac{F}{\pi LE^{*}}\left(1+\ln\frac{\pi E^{*}L^{3}}{RF}\right)=\frac{F}{\pi LE^{*}}\left(1+\ln\frac{4L^{2}}{b^{2}}\right) \tag{2}$$

where E^{*} is effective elastic modulus and equal to:

$$\frac{1}{E^{*}}=\frac{1-\nu_{1}^{2}}{E_{1}}+\frac{1-\nu_{2}^{2}}{E_{2}}\,. \tag{3}$$

with E_1 and E_2 are elastic module of contacting bodies, ν_1 and ν_2 are Poisson's ratio. Later Johnson and other authors gave other forms of force-displacement e.g.:

$$d=\frac{F}{\pi LE^{*}}\left(\ln\frac{4\pi E^{*}LR}{F}-const\right) \tag{4}$$

where $const$=1 in [4], 0.72 and 0.572 in others [13].

Correspondingly, the experiment investigation consisting of compression of parallel cylinders or indenting a cylinder into an elastic body is carried out in [11, 14]. Empirical equations of load-displacement are provided to verify theoretical solutions. In Thwaite's compression test [15] of a contact between a cylinder and a half-space, the comparison of slopes (or contact stiffness) shows that the solution (2) is the closest to the experimental results. In Kunz's experimental investigation [14], it is found that the approach of parallel cylinders is proportional to the loading force: $F=cE^*Ld$, where c is constant c=0.175.

In the last few decades, some numerical studies of the finite length line contact have been carried out to investigate the effect of contact edge and bone shape of the contact area and on stress distribution [16, 17]. However, a more precise solution for the line contact is rarely provided. Recently an analytical solution for contact problem of toroidal indenter is given by Argatov et al. [18] and is validated numerically by the boundary element method. In this paper we propose an analytical approximation of contact stiffness of a rigid cylinder and an elastic half space based on the results of [18]. While we overtake the general form of solution, we let some parameters free and determine them finally by numerical simulation of indentation test using the boundary element method.

2. Effective MDR-Profile for a Finite Length Lying Cylinder

2.1. Analytical approximation based on an asymptotic solution

The main physical result of this paper will be the dependence of normal force on the indentation depth for a contact between an elastic half-space and a "lying" cylinder (with the axis parallel to the surface of the half-space.) However, we will "pack" this dependence in the terms of the Method of Dimensionality Reduction (MDR) [19] where the whole information about the system is compressed into effective plane profile $g(x)$. The advantage of this presentation is that $g(x)$ can be used not only to easy reconstruct the dependency of the normal force on the indentation depth but also to solve a variety of other related problems such as tangential contact problem with friction in the interface, adhesive contact problem, and contact of visco-elastic bodies. In this sense, $g(x)$ is, so to say, the "visiting card" of the profile in question which allows multi-purpose use.

Note that the possibility of mapping three-dimensional contacts onto contacts with elastic foundation is well known for axis-symmetric indenters with compact contact area [19]. Less known is that the same concept can also be used to arbitrary other profiles, as e.g. of a torus (not compact contact area) or a rough surface. The corresponding proof as well as examples of MDR-profiles for a number of non-axisymmetric contacts can be found in [18] and [20]. Profile $g(x)$ determines straightforwardly force-indentation dependence $F(d)$. Thus the information content of both dependencies is equal: one can either determine $F(d)$ from $g(x)$ or $g(x)$ from $F(d)$. Even if the information content of both the functions is the same, it is more convenient to have $g(x)$ as it allows to solve much more various problems than $F(d)$.

In [20] the explicit procedure of "extracting" profile $g(x)$ from dependency $F(d)$ is described. The procedure is very trivial: from known dependency $F(d)$ one first determines differential contact stiffness $k_n(d)=\mathrm{d}F(d)/\mathrm{d}d$ and then determines the dependence of d as function of variable $x=k_n/(2E^*)$. Dependency $d(x)$ is exactly searched-for function $g(x)$. In the present paper, this procedure is carried out numerically: first, dependency $F(d)$ is determined by direct simulation using the boundary element method. Subsequently, the described procedure is applied to extract $g(x)$. Finally, numerically found profile $g(x)$ is approximated analytically.

For the analytical approximation we use the form of $g(x)$ found in [18] for indentation of a torus. In [18], it is derived by an asymptotic analysis and verified through BEM simulations. The 1D profile for toroidal indenter is given by:

$$g(x)=\frac{R'^2}{4\rho}\left(\frac{\pi^2 R'}{x}+1\right)\exp\left(8\ln 2-\frac{\pi^2 R'}{x}\right). \tag{5}$$

Here, R' is the distance from the center of the torus tube to the center of the torus, ρ is the radius of the torus tube.

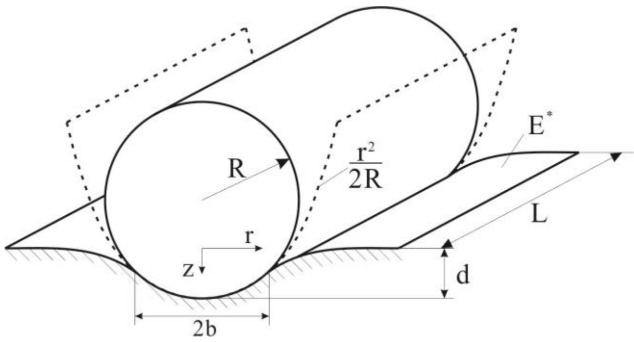

Fig. 1 A rigid cylinder lying on an elastic half space

The contact of the torus is very similar to that of a “lying” cylinder: both contacts are basically line ones and thus two-dimensional contacts whose logarithmic divergence is cut at some distance. For the torus, the role of the cut-off length plays the radius of the torus, while in the case of the lying cylinder this is the length of the cylinder. Equation (5) found for the torus thus can be used for lying cylinder with radius R and length L (Fig. 1) just by replacing $R'\to L$ and $\rho\to R$. The differences in two configurations are taken into account by introducing two coefficients c_1 and c_2 which in the case of the torus are equal to 1, but in the case a lying cylinder are allowed to take some other values:

$$g(x)=\frac{L^2}{4R}\left(c_1\cdot\frac{\pi^2 L}{x}+1\right)\exp\left(c_2\cdot 8\ln 2-c_1\cdot\frac{\pi^2 L}{x}\right). \tag{6}$$

In a more compact form Eq. (6) can be rewritten as:

$$g(x)=\beta\frac{L^2}{R}\left(\frac{\alpha L}{x}+1\right)\exp\left(-\frac{\alpha L}{x}\right) \tag{7}$$

where we have introduced two other fitting coefficients α and β (instead of c_1 and c_2). Introducing dimensionless parameters:

$$\tilde{x}=\frac{x}{L} \text{ and } \tilde{g}(\tilde{x})=\frac{g(x)R}{L^2}, \tag{8}$$

Eq. (7) can be written in the dimensionless form:

$$\tilde{g}(\tilde{x}) = \beta\left(\frac{\alpha}{\tilde{x}}+1\right)\exp\left(-\frac{\alpha}{\tilde{x}}\right) . \tag{9}$$

2.2. Numerical simulation of the indentation test

Two unknown coefficients α and β in Eq. (7) will be determined by numerical simulation of indentation test using the boundary element method which was developed by Pohrt, Li and Popov for various 3D contact problems including the partial sliding contact [21] and adhesive contact [22, 23].

In the simulation, the whole simulation area was divided into 512×512 rectangular elements. The rigid cylinder was modeled as parabolic indenter $f(y)=y^2/(2R)$, where y is in-plane coordinate perpendicular to the axis of the cylinder. The cylinder was indented in an elastic half space with controlled indentation depth in 100 steps from zero (first contact) to $0.15R$. The pressure distribution as well as the normal load and normal contact stiffness were calculated in each step of indentation. One example of contact configuration and pressure distribution is shown in Fig. 2. The concentration of pressure at the contact edge can be clearly observed in Fig. 2b.

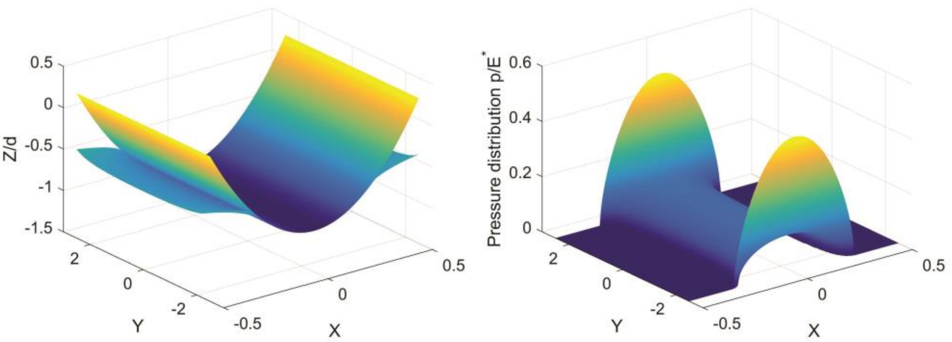

(a) (b)

Fig. 2 An example of numerical simulation for L/R=5 and d=0.1R: (a) contact state (b) pressure distribution

3. Results and Discussion

We have performed indentation simulations for cylinders with 29 increasing values of L/R ranging from L/R =0.1 to 20 (10 linearly increasing L/R from 0.1 to 1, and 19 from 2 to 20). Resulting MDR-profiles $g(x)$ are shown with crosses in Fig. 3a. In Fig. 3b, all curves are plotted in dimensionless form in coordinates (8). It is seen that all crosses for different L/R collapse to a single curve thus confirming the basic structure of the solution:

$$g(x) = \frac{L^2}{R}\Phi\left(\frac{x}{L}\right) . \tag{10}$$

Fig. 3b provides the numerically determined form of function Φ(.).

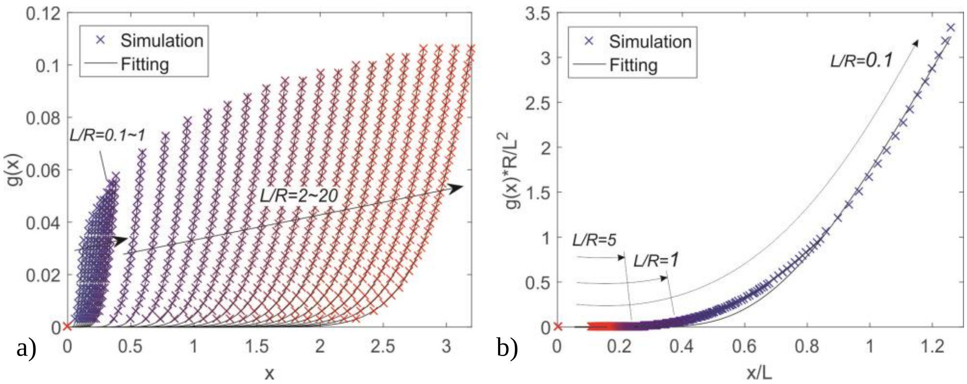

Fig. 3 1D profile of lying cylinder calculated by BEM simulation (cross) and fitting with Eq. (7)

In the following, we provide analytical approximation for this function on the basis of Eq (9). The values of coefficients α and β are calculated by the method of least squares. The agreement of fitting (black solid lines) with numerical simulation can be seen in Fig. 3. Values of α and β are presented in Fig. 4, where we can see that both factors are almost constant for large ratios of L/R but change significantly for small ratios. We thus discuss the cases of "long cylinders" and "short cylinders" separately.

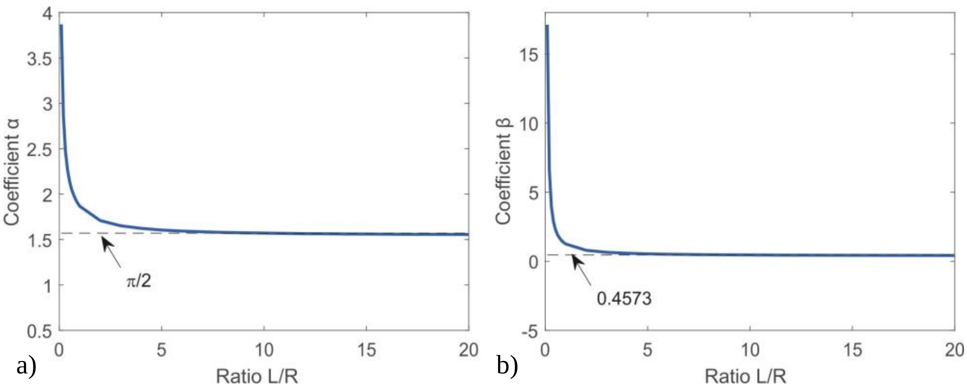

Fig. 4 Values of coefficients of α (a) and β (b) for different ratios of L/R obtained by fitting of Eq. (7) with numerical results

(a) Large ratio L/R ("long cylinder")

From Fig. 4, one can see that α and β for larger L/R are almost constant: $\alpha=\pi/2$ and $\beta=0.4537$. Thus, for large ratios in the range of about $L/R \geq 5$ we can give the following approximation:

$$g(x) = 0.4573\frac{L^2}{R}\left(\frac{\pi}{2}\frac{L}{x}+1\right)\exp\left(-\frac{\pi}{2}\frac{L}{x}\right), \quad \text{for } L/R \geq 5\,, \tag{11}$$

or in the dimensionless form:

$$\tilde{g}(\tilde{x}) = 0.4573\left(\frac{\pi}{2\tilde{x}}+1\right)\exp\left(-\frac{\pi}{2\tilde{x}}\right), \text{ for } L/R \geq 5 \ . \tag{12}$$

Numerical results and analytical approximations (11) and (12) in this range of L/R are shown in Fig. 5.

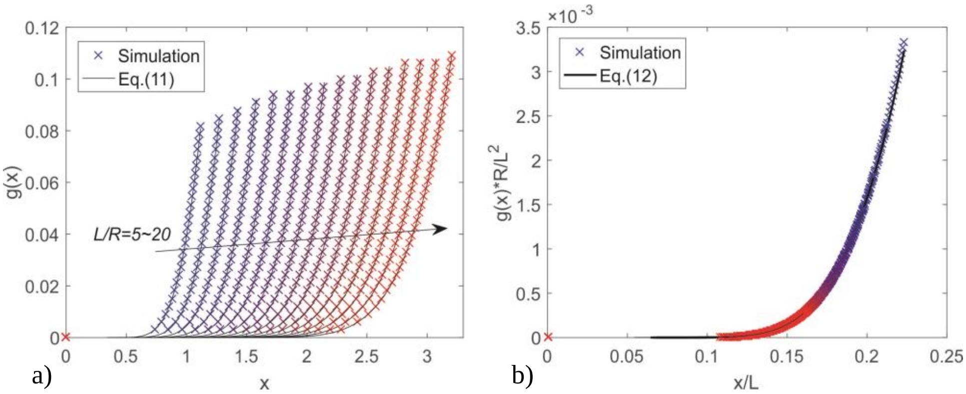

Fig. 5 1D profile of cylinder for larger ratios of *L/R*:
(a) for different *L/R* (b) in dimensionless form

(b) Small ratio of L/R ("short cylinder")

In practical applications, many line-contact machine elements are thin plates meaning a small value of *L/R*, as e.g. cams. The results of numerical simulation and fitting for *L/R* =0.1~4 are clearly shown in Fig. 6. Coefficients α and β in this range are different (Fig. 4); however, from the subplot of Fig. 6b we can find that the fittings agree with the numerical results also well, except for very small *L/R* (=0.1 or 0.2) (subplot in Fig. 6b), so we list their values in Tab. 1 for the further studies.

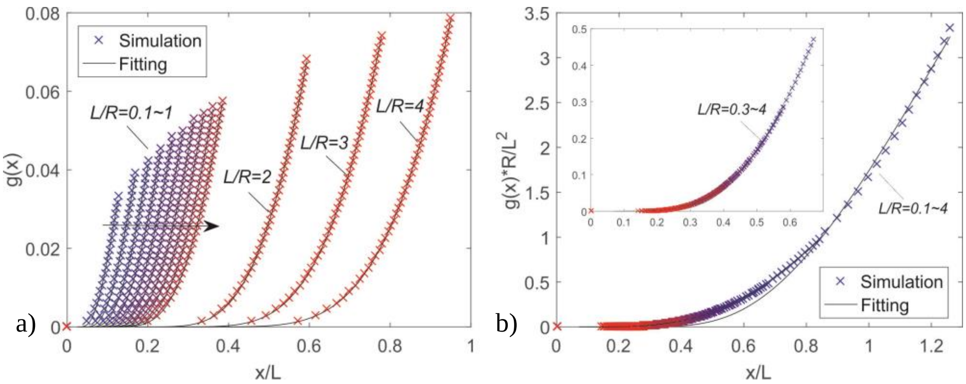

Fig. 6 1D profile of cylinder for small ratios of *L/R*:
(a) for different *L/R* (b) in dimensionless form

Table 1 Values of coefficients α and β for small *L/R*

L/R	*A*	β	*L/R*	*A*	β	*L/R*	α	β
0.1	3.8695	17.1183	0.6	2.0528	1.9139	2	1.7086	0.7936
0.2	2.8664	6.6132	0.7	1.9928	1.6847	3	1.6518	0.6495
0.3	2.4734	3.9560	0.8	1.9400	1.4963	4	1.6231	0.5799
0.4	2.2714	2.8770	0.9	1.8996	1.3589	5	1.6048	0.5376
0.5	2.1455	2.2975	1	1.8668	1.2517	6	1.5930	0.5091

Finally, let us compare our results with those following from Eq. (2). Differentiation of the force with respect to the indentation depth provides the normal contact stiffness:

$$k_n = \pi L E^* \ln \frac{RF}{\pi E^* L^3} \quad . \tag{13}$$

Together with relation (2) we can obtain 1D profile $g(x)$, which has also a dimensionless form similar to Eq. (12). This dimensionless form is shown with a dashed line in Fig. 7. One can see that it differs substantially from the "numerically exact" result found in the present paper and plotted in Fig. 7 with a bold line.

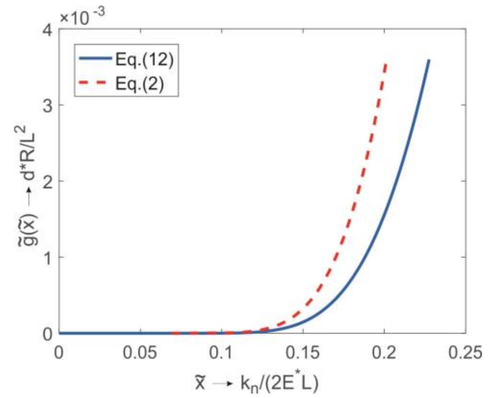

Fig. 7 Comparison of 1D profile obtained from existing solution and in this paper

4. Conclusion

We have numerically simulated indentation of the finite-length cylinder lying on an elastic half space. The ratio of the cylinder's length and radius was varied in a wide range from a thin disk (ratio 0.1) to a long pole (ratio 20). Based on the results of numerical simulation, the equivalent MDR-profiles containing the whole information about the contact problem was "extracted" and subsequently approximated analytically using an equation inspired by an asymptotic solution of the contact problem. For large length-to-radius ratios (larger than about 5), the fitting coefficients are almost constant and a general form with high accuracy is provided in a closed analytical form. For small length-to-radius ratios, analytical solution is provided which contains two constants provided in the form of a table. Comparison of the present solution with the already available analytical approximation shows that the present solution is much more precise.

REFERENCES

1. Harris, T.A., 2001, *Rolling bearing analysis*, John Wiley and Sons, New York.
2. Norton, R., 2009, *Cam Design and Manufacturing Handbook*, Industrial Press.
3. Popov, V.L., 2010, *Contact Mechanics and Friction: Physical Principles and Applications*, Springer, Berlin.
4. Jonson, K.L., 1985, *Contact Mechanics*, Cambridge University Press, Cambridge.
5. Landau, L.D., Lifshitz, E.M., 1970, *Theory of Elasticity*, Course of Theoretical Physics.
6. Venner, C.H., Lubrecht, A.A., 1994, *Transient Analysis of Surface Features in an EHL Line Contact in the Case of Sliding*, Journal of Tribology, 116(2), pp. 186–193.
7. Hamrock, B.J., Schmid, S.R., Jacobson, B.O., 2004, *Fundamentals of Fluid Film Lubrication*, Marcel Dekker, New York.
8. Prescott, J., 1946, *Applied Elasticity*, Dover Publications.
9. Thomas, H.R., Hoersch, V.A., 1930, *Stresses Due to the Pressure of One Elastic Solid Upon Another: A Report of an Investigation Conducted by the Engineering Experiment Station*, University of Illinois in Cooperation with the Utilities Research Commission.
10. Lundberg, G., 1939, *Elastische Berührung zweier Halbräume*, Forschung auf dem Gebiet des Ingenieurwesens A, 10(5), pp. 201–211.
11. Norden, B.N., 1973, *On the compression of a cylinder in contact with a plane surface*, National Bureau of Standards, Washington D.C.
12. Puttock, M.J., Thwaite, E.G., 1969, *Elastic Compression of Spheres and Cylinders at Point and Line Contact*, National Standards Laboratory.
13. Nakhatakyan, F.G., 2011, *Precise solution of Hertz contact problem for circular cylinders with parallel axes*, Russian Engineering Research, 31(3), pp. 193–196.
14. Kunz, J., de Maria, E., 2002, *Die Abplattung im Kontaktproblem paralleler Zylinder*, Forschung Im Ingenieurwesen, 67(4), pp. 146–156.
15. Thwaite, E.G., 1969, *A precise measurement of the compression of a cylinder in contact with a flat surface*, Journal of Physics E: Scientific Instruments, 2(1), pp. 79–82.
16. Glovnea, M., Diaconescu, E., 2004, *New Investigations of Finite Length Line Contact*, In ASME Proceedings, Special Symposia on Contact Mechanics, pp. 147–152.
17. Najjari, M., Guilbault, R., 2014, *Modeling the edge contact effect of finite contact lines on subsurface stresses*, Tribology International, 77, pp. 78–85.
18. Argatov, I., Heß, M., Pohrt, R., Popov, V.L., 2016, *The extension of the method of dimensionality reduction to non-compact and non-axisymmetric contacts*, ZAMM Journal of Applied Mathematics and Mechanics, 96(10), pp. 1144–1155.
19. Popov, V.L., Heß, M., 2015, *Method of Dimensionality Reduction in Contact Mechanics and Friction*, Springer, Berlin.
20. Popov, V.L., Pohrt, R., Heß, M., 2016, *General procedure for solution of contact problems under dynamic normal and tangential loading based on the known solution of normal contact problem*, The Journal of Strain Analysis for Engineering Design, 51(4), pp. 247–255.
21. Pohrt, R. Li, Q., 2014, *Complete Boundary Element Formulation for Normal and Tangential Contact Problems*, Physical Mesomechanics, 17(4), pp. 334–340.
22. Pohrt, R., Popov, V.L., 2015, *Adhesive contact simulation of elastic solids using local mesh-dependent detachment criterion in boundary elements method*, Facta Universitatis, Series: Mechanical Engineering, 13(1), pp. 3–10.
23. Li, Q., Popov, V.L., 2016, *Boundary element method for normal non-adhesive and adhesive contacts of power-law graded elastic materials*, arXiv:1612.08395.